iScience

CellPress

Article

High-Efficiency Multi-site Genomic Editing of *Pseudomonas putida* through Thermoinducible ssDNA Recombineering

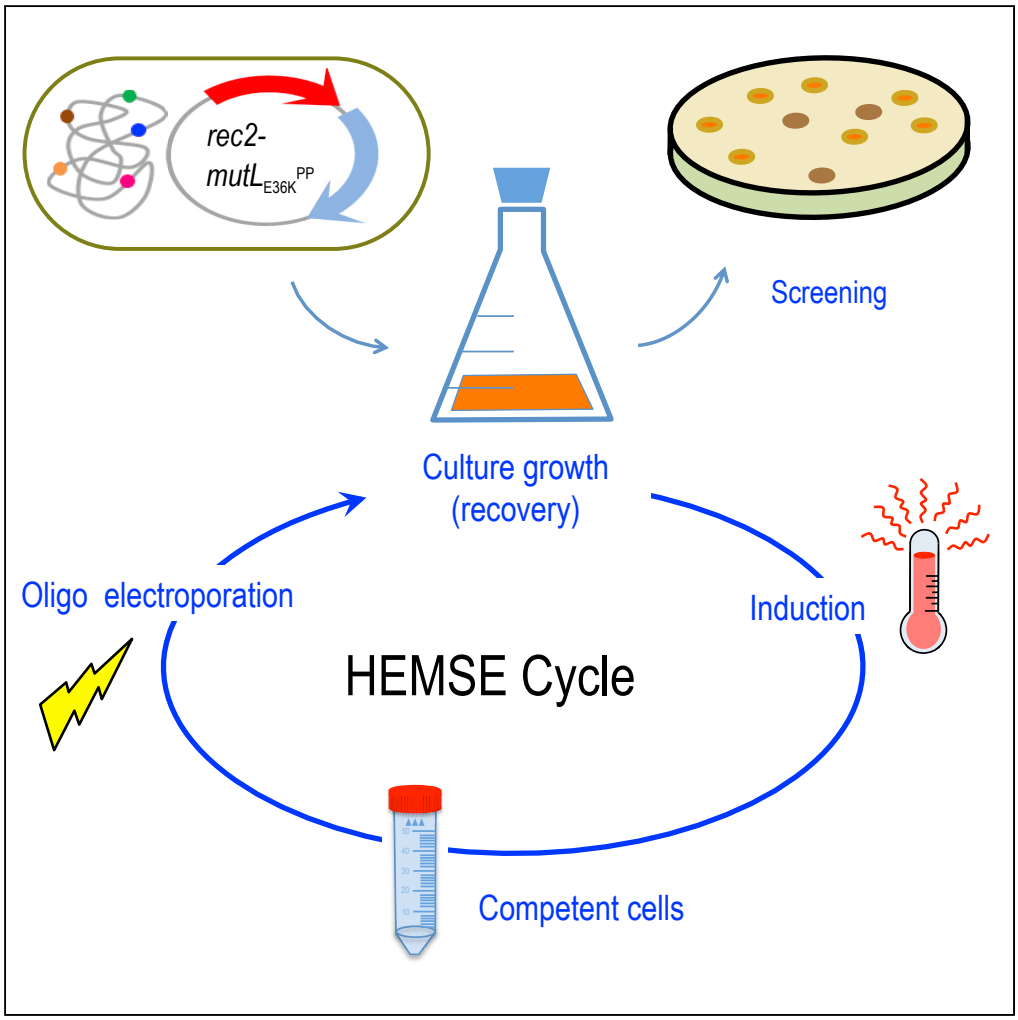

Tomas Aparicio, Akos Nyerges, Esteban Martínez-García, Víctor de Lorenzo

emartinez@cnb.csic.es (E.M.-G.)
vdlorenzo@cnb.csic.es (V.d.L.)

HIGHLIGHTS

Pseudomonas putida is a useful Synthetic Biology chassis for metabolic engineering

Co-expression of Rec2 recombinase and mutLE36K allele empowers ssDNA recombineering

Cyclic DNA replication fork invasion causes up to 10% single-site mutation frequency

The experimental HEMSE pipeline eases multi-site genome editing of *P. putida*

Aparicio et al., iScience *23*, 100946
March 27, 2020
https://doi.org/10.1016/j.isci.2020.100946

iScience

CellPress

Article

High-Efficiency Multi-site Genomic Editing of *Pseudomonas putida* through Thermoinducible ssDNA Recombineering

Tomas Aparicio,[1] Akos Nyerges,[2,3] Esteban Martínez-García,[1,*] and Víctor de Lorenzo[1,4,*]

SUMMARY

Application of single-stranded DNA recombineering for genome editing of species other than enterobacteria is limited by the efficiency of the recombinase and the action of endogenous mismatch repair (MMR) systems. In this work we have set up a genetic system for entering multiple changes in the chromosome of the biotechnologically relevant strain EM42 of *Pseudomononas putida*. To this end high-level heat-inducible co-transcription of the *rec2* recombinase and *P. putida*'s allele $mutL_{E36K}^{PP}$ was designed under the control of the P_L/cI857 system. Cycles of short thermal shifts followed by transformation with a suite of mutagenic oligos delivered different types of genomic changes at frequencies up to 10% per single modification. The same approach was instrumental to super-diversify short chromosomal portions for creating libraries of functional genomic segments—e.g., ribosomal-binding sites. These results enabled multiplexing of genome engineering of *P. putida*, as required for metabolic reprogramming of this important synthetic biology chassis.

INTRODUCTION

DNA recombineering was first developed in the early 2000s (Datsenko and Wanner, 2000; Yu et al., 2000) as a genetic technology for replacing genomic segments of *E. coli* with synthetic double-stranded (ds) DNA by means of the DNA exchange mechanism brought about by the Red system of phage lambda. Although the native approach involves three proteins (a β-recombinase, an exonuclease, and the γ protein, which protects free ds ends of DNA from degradation by RecBCD), it turned out that the Red-β protein sufficed to promote invasion of the replication fork by single-stranded (ss) oligonucleotides incorporated as Okazaki fragments (Ellis et al., 2001). If such oligonucleotides were designed to carry mutations, the resulting changes could be inherited at considerable frequencies upon subsequent rounds of DNA segregation. The key value of this approach is that by using cocktails of mutagenic oligonucleotides and either manual or automated cycles of Red expression/oligonucleotide transformation one can enter simultaneous changes in many genomic sites and/or saturate given DNA stretches with specific or random mutations (Wang et al., 2009; Nyerges et al., 2016, 2018). This technology gave rise to MAGE (multiplex automated genome engineering) in *E. coli*, a cycled and multiplexed application of recombineering that exploits the capabilities of the Red system for large-scale reprogramming of cells, i.e., metabolic engineering of lycopene production (Wang et al., 2009) or genome-wide codon replacements (Isaacs et al., 2011). These methods have been improved further by using host strains transiently disabled in mismatch repair (MMR) and by enriching mutants through Cas9/guide RNA-based counterselection of wild-type sequences (Costantino and Court, 2003; Jiang et al., 2013; Nyerges et al., 2014, 2016; Ronda et al., 2016; Oesterle et al., 2017). These technologies work well in *E. coli*, whereas they are difficult to transplant directly to non-enteric bacteria. Yet, their applicability to species such as *Pseudomonas putida* has a special interest because of the value of environmental microorganisms as useful platforms for metabolic engineering (Nikel et al., 2014; Nikel et al., 2016; Martínez-García and de Lorenzo, 2019). Attempts of functional expression of the lambda Red system in various species of *Pseudomonas* have been reported, but recombination frequencies were low in the absence of selection (Lesic and Rahme, 2008; Liang and Liu, 2010; Luo et al., 2016; Chen et al., 2018; Yin et al., 2019). Red-like counterparts found in *Pseudomonas* prophages have been more successful to the same ends. For example, the RecET recombinase/exonuclease pair of *P. syringae* has been instrumental for executing a suite of manipulations in this species (Swingle et al., 2010a; Bao et al., 2012). Furthermore, bioinformatic mining of *Pseudomonas*-borne recombinases from known protein families (i.e., Redβ, ERF, GP2.5, SAK, and SAK4; Lopes et al., 2010) followed by experimental validation of the most promising in a standardized recombineering test exposed two new enzymes (Ssr and Rec2: Aparicio et al., 2016; Ricaurte et al., 2018; Aparicio et al., 2020). These

[1]Systems and Synthetic Biology Program, Centro Nacional de Biotecnología (CNB-CSIC), Campus de Cantoblanco, Madrid 28049, Spain

[2]Synthetic and Systems Biology Unit, Institute of Biochemistry, Biological Research Centre, Szeged 6726, Hungary

[3]Present address: Harvard Medical School, Boston, MA 02115, USA

[4]Lead Contact

*Correspondence: emartinez@cnb.csic.es (E.M.-G.), vdlorenzo@cnb.csic.es (V.d.L.)

https://doi.org/10.1016/j.isci.2020.100946

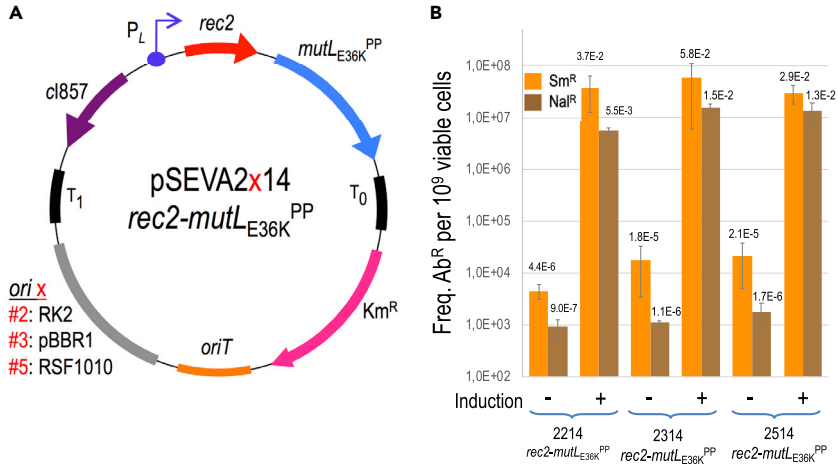

Figure 1. Influence of Plasmid Copy Number on the Editing Efficiency of the Heat-Induced *rec2-mutL*$_{E36K}^{PP}$ Genes

(A) Genetic map and structure of plasmids used in this study. The figure shows the plasmids tested, all having the same elements with the exception of the origin of replication, represented with "x." T_0 and T_1, transcriptional terminators; Km, kanamycin resistance gene; *ori*T, origin of transfer; cI857-P_L, temperature-inducible expression system; *rec2*, recombinase; *mutL*$_{E36K}^{PP}$, dominant-negative allele of *mutL*; *ori* x (origin of replication): #2, RK2 (low copy number); #3, pBBR1 (medium copy number); #5, RSF1010 (medium-high copy number). Pictures are not drawn to scale.

(B) Recombineering assays with *P. putida* EM42: the strain harboring each pSEVA2x14-*rec2-mutL*$_{E36K}^{PP}$ variant was subjected to recombineering with oligos SR and NR upon heat induction of the cI857-P_L expression system and without induction. After overnight recovery, culture dilutions were plated on LB-Sm (SR oligo) and LB-Nal (NR oligo) to estimate the number of allelic changes. Culture dilutions plated on LB allowed viable cell counting. Column values represent mean recombineering frequencies (mutants per 10^9 viable cells) of two independent experiments with the standard deviation.

recombinases delivered a comparatively high level of activity in the reference strains *P. putida* KT2440 and its genome-reduced derivative *P. putida* EM42. Still, numbers were way below those reported for *E. coli*. Furthermore, the action of the endogenous MMR system of this bacterium impeded single-nucleotide changes (i.e., A to T, mismatch A:A) that were efficiently fixed by the indigenous *mutS/mutL* device (Aparicio et al., 2016, 2019b).

In this work we have set out to overcome the above-mentioned bottlenecks to efficacious recombineering in *P. putida*. The approach builds on the apparently superior ability of the Rec2 recombinase to promote DNA annealing with exogenous synthetic oligonucleotides during chromosomal replication. By playing with a stringent expression system for *rec2*, applying multiple cycles of recombinase production/oligonucleotide transformation, and reversibly inhibiting the MMR system during a limited time window we report in the following discussion high-fidelity recombination frequencies that approach those achieved with the archetypal Red-based system (Datsenko and Wanner, 2000). This opens genome editing possibilities in this environmental bacterium that were thus far limited to strains of *E. coli*, closely related enteric species (Nyerges et al., 2018; Szili et al., 2019), and some lactic acid bacteria (van Pijkeren et al., 2012).

RESULTS

Optimization of Rec2 and MutL$_{E36K}^{PP}$ Delivery for ssDNA Recombineering

The bicistronic gene cassette of pSEVA2514-*rec2-mutL*$_{E36K}^{PP}$ (Figure 1A) was developed earlier for examining the hierarchy of recognition of different types of single-nucleotide mispairs by the native MMR system of *P. putida* (Aparicio et al., 2019b). In this construct *rec2* and *mutL*$_{E36K}^{PP}$ were placed under the control of the thermo-inducible P_L/cI857 system, in which the product of cI857 represses the P_L promoter at 30°C but becomes inactivated at 42°C, triggering the expression of the genes after a short thermal shift. During the course of that work, we noticed that a short, transient thermal induction of the Rec2 recombinase increased very significantly ssDNA recombineering (~1 order of magnitude) when compared with the same with an expression device responsive to 3-methylbenzoate (i.e., *xylS*/P*m*). Although the reason for this improvement is not entirely clear, it may have resulted from (1) the short-lived, high-level transcription of the otherwise toxic recombinase—when compared with the permanent hyperexpression caused by the chemically inducible system; (2) thermal inactivation of ssDNA nucleases and thus

improved survival of the mutagenic oligonucleotides *in vivo;* or (3) a combination of both. In any case, the average frequency of single-base replacements in just one single-shot recombineering test was in the range of 1×10^{-2} mutants per viable cell. This was high when compared with previous recombineering efforts in this bacterium (Aparicio et al., 2016) but still low for identifying mutations without a selectable phenotype. We, however, speculated that by multi-cycling the procedure with short thermal pulses of recombinase induction and transformation with mutagenic oligos, such frequencies could be added at each cycle, eventually resulting in high nucleotide replacement rates. A second realization (Aparicio et al., 2019b) was that transient co-expression of the dominant allele $MutL_{E36K}^{PP}$ of the MMR system of *P. putida* along with the *rec2* gene in plasmid pSEVA2514-*rec2*-$mutL_{E36K}^{PP}$ (Figure 1) virtually eliminated recognition of any type of base mispairings in DNA. This allowed entering all classes of nucleotide replacements that would otherwise be conditioned by MMR—without triggering a general mutagenic regime. Yet, note that both activities (Rec2 and $MutL_{E36K}^{PP}$) were delivered *in vivo* with a high-copy-number vector with an origin or replication (RSF1010) of unknown thermal sensitivity. This may result in some instability upon thermal cycling of the procedure for boosting recombineering efficiency (see below). To determine the best plasmid frame for *rec2*-$mutL_{E36K}^{PP}$ transient expression, the cognate DNA segment was recloned in vectors pSEVA2214 (RK2 origin or replication, low copy number) and pSEVA2314 (pBBR1 origin, medium copy number) as shown in Figure 1A. Recombineering tests were then carried out with oligonucleotide NR, which generated a double mutation in *gyrA* endowing resistance to nalidixic acid (Nal^R) by means of two MMR-sensitive changes G → A and C → T. In parallel, another MMR-insensitive change A → C was also tested with oligonucleotide SR that mutated *rpsL* for making cells resistant to streptomycin (Sm^R), and recombineering assays were run in non-induced and heat-induced cultures. The results of this test indicated that thermal induction of *rec2* and $mutL_{E36K}^{PP}$ genes enhances recombineering by 3–4 logs with efficiencies in the range of 1×10^{-2} mutants/viable cell for the three plasmids assayed. Performance comparison points to pSEVA2314-*rec2*-$mutL_{E36K}^{PP}$ as the preferred construct of reference for the multi-site mutagenesis platform presented in the following discussion. On the basis of this we set out to re-create in *P. putida* the same conditions that enabled implementation in *E. coli* of high-efficiency ssDNA recombineering protocols such as MAGE (Wang et al., 2009), DIvERGE (directed evolution with random genomic mutations; Nyerges et al., 2018), and pORTMAGE (portable MAGE; Nyerges et al., 2016)—and thus expand frontline genomic editing methods toward this environmentally and industrially important bacterium.

Cyclic Pulses of rec2/$mutL_{E36K}^{PP}$ Expression Enable a High Level of Single-Nucleotide Substitutions

The first issue at stake was determining the frequencies of mutations caused by using a cocktail of oligonucleotides targeting five genes representative of diverse genomic locations, different types of nucleotide changes, and associated or not with selectable traits upon multiple ssDNA recombineering cycles. The genes at stake, their position in the chromosomal map, the cognate phenotypes, and the type of replacements brought about by the corresponding mutagenic ssDNAs are summarized in Figure 2. They were all designed to pair sequences in the lagging strand of the replication fork in each of the replichores of the *P. putida* genome according to Aparicio et al. (2016). Note that the experiments were run with *P. putida* EM42, not with the archetypal strain KT2440. This is because it is a $recA^+$ derivative of the EM383 genome-streamlined variant that has higher endogenous levels of ATP and NAD(P)H and has thus become a preferred metabolic engineering platform (Martínez-García et al., 2014). Moreover, the modifications entered in *P putida* EM42 make this strain more tolerant to pulses of high temperature (Aparicio et al., 2019a), as repeatedly applied throughout this work (see later). The cyclic recombineering protocol (see Transparent Methods for details) is summarized in Figure 3, and it basically involves four steps: (1) growing cells, (2) triggering thermal induction of *rec2* and $mutL_{E36K}^{PP}$ genes by a short heat shock, (3) preparing competent cells for electroporation with the mutagenic oligonucleotides, and (4) recovering the culture for a new cycle.

The results of applying multiple recombineering cycles to *P. putida* EM42 (pSEVA2314-*rec2*-$mutL_{E36K}^{PP}$) with the oligonucleotides listed in Figure 2B are shown in Figure 4A. Note that the frequencies of mutant appearance increased during the runs from 2.8×10^{-3} (1 cycle) to 9.3×10^{-2} (10 cycles) in the case of *gyrA*, and from 4.8×10^{-2} to 2.0×10^{-1} for *pyrF* under the same conditions. In the best-case scenario (i.e., gene *rpsL*), the frequencies multiplied by 24-fold, reaching a remarkable 21%. After the 10th cycle, these figures are thus close to the rates reported in *E. coli* with the archetypal Red-β system of phage lambda and also to the theoretical limit of recombineering frequencies (25%) that stems from segregation of

A

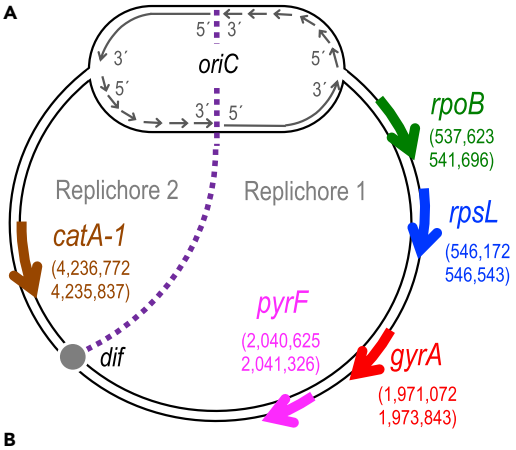

B

Oligo	Target gene (locus)	Allelic change	MMR sensitivity	Phenotype
SR	*rpsL* (PP_0449)	Single nt.	Low	Sm^R
NR	*gyrA* (PP_1767)	Two nt.	High	Nal^R
RR	*rpoB* (PP_0447)	Single nt.	High	Rif^R
PR	*pyrF* (PP_1815)	Single nt.	Low	$5FOA^R/Ura^-$
CR	*catA-I* (PP_3713)	Insertion 3 Stops	---	Brown

Figure 2. Target Genes and Recombineering Oligonucleotides Used for HEMSE

(A) The five genes selected as targets for recombineering are represented in the chromosomal map of *P. putida* KT2440 with gene coordinates and strand orientation. *oriC* and *dif* regions are shown to define the two replichores in the genomic map. Pictures are not drawn to scale.

(B) The main features of recombineering oligonucleotides used to assay HEMSE are shown: name of oligo, target gene with its locus tag, type of allelic replacement, level of MMR sensitivity of the allelic changes, and the cognate phenotypes produced. See Tables S1 and S3 for additional information.

one allelic change after two rounds of genome replication (Wang et al., 2009; Nyerges et al., 2016). It is worth mentioning that control strain *P. putida* EM42 harboring insertless vector pSEVA2314—but transformed with the same mutagenic oligonucleotides—gave rise to recombineering frequencies $\sim 1 \times 10^{-5}/1 \times 10^{-6}$ mutants/viable cells per cycle for single changes (Figure S1). Given that these background levels are higher with thermal induction than with chemical induction (Ricaurte et al., 2018), it is plausible that heat shock intrinsically improves recombineering regardless of the action of heterologous recombinases. As a matter of fact, purely endogenous ssDNA recombineering at significant frequencies has been reported in a variety of Gram-negative bacteria, including *E. coli* and *Pseudomonas syringae* (Swingle et al., 2010b), a fact that plays in our favor for establishing the methodology in *P. putida*.

The most remarkable outcome of the operations shown in Figure 4A was that such high figures enabled manual screening of inconspicuous mutations, thus avoiding the need of adding a genetic counterselection device (e.g., CRISPR/Cas9) for identifying rare changes. As these results accredited the value of multi-cycling thermoinduction of the bicistronic *rec2-mutL*$_{E36K}^{PP}$ operon of pSEVA2314-*rec2-mutL*$_{E36K}^{PP}$ for raising ssDNA recombineering efficiency, the next obvious question was whether the high figures could afford simultaneous multi-site genomic editing with mixtures of mutagenic oligos, in a fashion reminiscent of the MAGE process available for *E. coli*.

Multi-site Editing of Non-Adjacent Genomic Locations

Given average individual mutation rates of 10% after 10 thermal recombineering cycles and assuming they are separately maintained when cells face a cocktail of mutagenic oligonucleotides one can

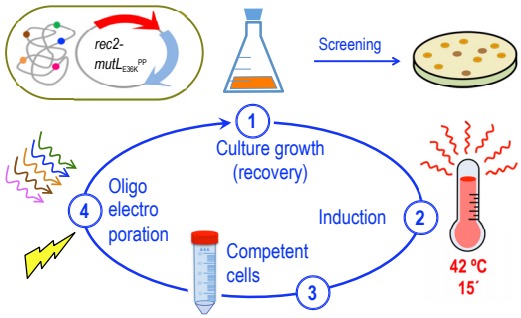

Figure 3. Scheme of HEMSE Cycle

The main steps of the procedure are depicted: cultures of *P. putida* EM42 (pSEVA2314-*rec2-mutL*$_{E36K}^{PP}$) grown at OD_{600} = 1.0 are induced by a heat shock at 42°C/15 min; then competent cells are prepared and transformed with recombineering oligonucleotides. After recovery on fresh media at 30°C/170 rpm, cultures enter into the next round of HEMSE by applying the induction step. Screening of allelic replacements within a given cycle is performed after recovery by plating culture dilutions on the appropriate solid media (see Transparent Methods for details).

predict frequencies of 1% double changes all the way to 0.001% mutants (1×10^{-5}) of genomes with all the five changes in the absence of any phenotypic advantage. To test this prediction, we subjected a culture of *P. putida* EM42 (pSEVA2314-*rec2-mutL*$_{E36K}^{PP}$) to 10 cycles of thermo-induced recombineering (see Transparent Methods) with re-transformation in each cycle with an equimolar mixture of oligos SR, NR, RR, PR, and CR (Figure 2B; Table S1) so that all possible changes could be entered in the same cells. Emergence of multiple (i.e., quadruple and quintuple) mutations in the population was then monitored at cycles I, V, and X and their frequencies recorded. Figure 4B shows the results of such a procedure. The data exposed a good match between the theoretical expectation of multiple changes and the actual figures, although the evolution of the mutation rates was not linear. At cycle #1, single changes showed recombineering frequencies barely below 1×10^{-2} mutants per viable cell. If we take that as a reference, theoretical frequencies of acquisition of four and five changes would be 1×10^{-8} and $1E^{-10}$ respectively, whereas the actual numbers were way higher (6×10^{-6} and 2×10^{-7}). By cycle #5, single changes reached average recombineering above 5×10^{-2}. The gross theoretical prediction for simultaneous appearance of four and five changes would be as low as 6×10^{-6} and 3×10^{-7}. Yet, again, the actual experiments yield 1.3×10^{-4} and 2.3×10^{-6} mutants per viable cell for quadruple and quintuple mutants. By cycle #10, however, the scenario was different. Single changes appeared at frequencies $\sim 1 \times 10^{-1}$, close to the theoretical maximum of recombineering efficiency (2.5×10^{-1}). In this case, predicted frequencies for four and five changes were 1×10^{-4} and 1×10^{-5}, which were very similar to the actual numbers delivered by the experiment, i.e., 2×10^{-4} and 6×10^{-6}.

The aforementioned results suggested that during the first five recombineering cycles a strong co-selection phenomenon occurs. Appearance of multiple mutations is 2–3 logs higher than expected, suggesting that cells undergoing ssDNA incorporation in specific loci are more prone to incorporate changes in other genomic locations. This phenomenon, which has been observed before (Carr et al., 2012; Gallagher et al., 2014), could be due to differences in the ability of single cells in a population to take up exogenous ssDNA upon electroporation. Regardless of the specific mechanisms, the results of Figure 4B show that multi-cycle recombineering boosts mutagenic frequencies through single to quintuple changes. Yet, whereas 10 cycles appear to reach saturation at single sites, it is plausible that additional runs could enrich further the population in multi-edited bacterial cells. Taken together, the experiments of Figure 4 document the power of the hereby described method for simultaneously targeting five genomic sites of *P. putida* for desired mutations. On this basis we propose to call the entire workflow high-efficiency multi-site genomic editing (or HEMSE). The method is conceptually comparable to MAGE developed for *E. coli* (Wang et al., 2009), but it lacks (thus far) the automation aspect.

As a growing culture of *P. putida* in lysogeny broth (LB) typically ranges from 10^8 to 10^9 cells/mL from early exponential to early stationary phase, we speculated that the maximum number of genes that could be edited in a HEMSE experiment of this sort with mixed oligos in the absence of any selective advantage or phenotypic screening could be $\sim$ 8–9. This is clearly not enough for massive changes of the sort necessary, e.g., for recoding a whole genome (Isaacs et al., 2011) or reassigning/erasing specific triplets

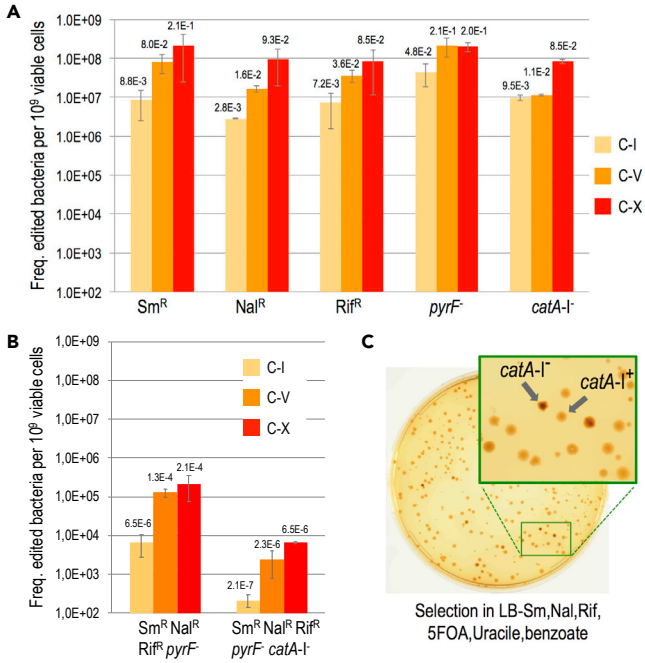

Figure 4. Editing Efficiencies HEMSE

(A) Editing efficiencies of single changes were assayed applying 10 cycles of HEMSE to *P. putida* EM42 (pSEVA2314-*rec2-mutL*$_{E36K}^{PP}$) using an equimolar mixture of oligos SR, NR, RR, PR, and CR. After recovery steps of cycles n° 1 (C-I), n° 5 (C-V), and n° 10 (C-X), appropriate dilutions of the cultures were plated on LB to estimate viable cells and also on LB solid media supplemented with Sm, Nal, Rif, 5FOA-Ura, or benzoate to enumerate allelic replacements. Colonies growing on Sm, Nal, Rif, or 5FOA-Ura were counted as allelic changes, whereas brown, catechol-accumulating colonies growing in LB-benzoate were counted as *catA*-I$^-$ clones (see phenotype in Figure S2). Recombineering frequencies of single replacements at each cycle were normalized to 10^9 viable cells, and the media of two independent replicas were plotted with standard deviations. Absolute recombineering frequencies (mutants per viable cell) are also depicted over the bars.

(B) From the same experiments, editing efficiencies of multiple changes were analyzed. Dilutions of C-I, C-V, and C-X were plated on LB-SmNalRif-5FOA-Ura and LB-SmNalRif-5FOA-Ura-benzoate solid media, allowing the estimation of, respectively, quadruple (Sm^R Nal^R Rif^R *pyrF*) and quintuple (Sm^R Nal^R Rif^R *pyrF*$^-$ *catA*-I$^-$) editions. Results are represented as in (A).

(C) A representative plate of quintuple screening at C-X is shown. The zoom-up shows colonies with the characteristic dark brown phenotype of *catA*-I$^-$ clones.

(Ostrov et al., 2016). Fortunately, in most typical metabolic engineering endeavors, the issue is not so much entering many defined mutations in given chromosomal sites but fostering the system to explore a solution space by letting it come up with many combinations—the most successful of which can be enriched and subject to further mutation rounds. This effect can be exacerbated if the mutagenic oligos boost the diversification of, e.g., regulatory sequences, so their combination generates fluctuations in the stoichiometry of a multi-gene pathway (Hueso-Gil et al., 2020)—or they create variants of the same protein with different activities by diversifying specific segments. The technical issue shared by all these scenarios is the focusing of the diversification in a defined sequence window of the genomic DNA. In this context the question is whether the above-described HEMSE is instrumental to this end also—as the recombineering-based method to the same end called DIvERGE is in *E. coli* and related enterobacteria (Nyerges et al., 2018).

Diversification of the SD Motif Context Creates New Functional RBSs in *P. putida*

To have a tractable proxy of generation *in vivo* of large libraries of functional DNA sequences in the *P. putida* genome, the experimental setup shown in Figure 5 was developed. In it, a Tn*7* mini-transposon vector was inserted with the *gfp* gene downstream of the constitutive promoter P$_{EM7}$ but lacking a recognizable Shine-Dalgarno (SD) sequence for translation initiation. The hybrid transposon was subsequently inserted in the cognate *att*Tn*7* site of the *P. putida* EM42 chromosome (see Transparent Methods) from which it was expectedly unable to produce any detectable fluorescence. The resulting strain (*P. putida* TA245, Table S2) was transformed with pSEVA2314-*rec2- mutL*$_{E36K}^{PP}$ and used in recombineering

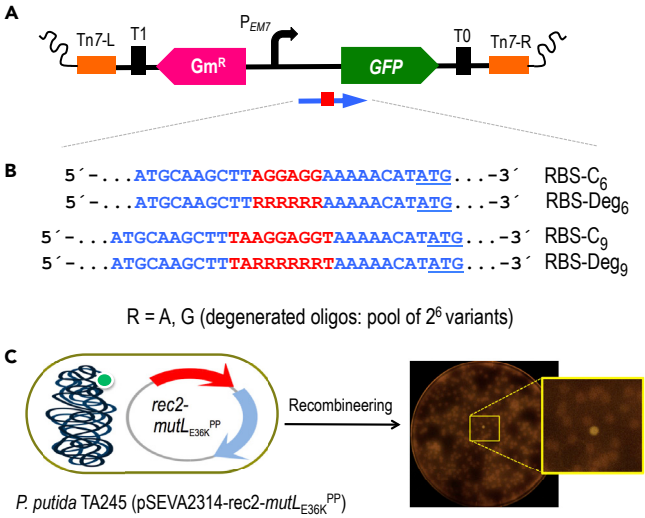

Figure 5. Diversification of the *gfp* Shine-Dalgarno Motif

(A) A mini-Tn*7* transposon bearing the *gfp* gene devoid of its original SD sequence and under the control of the constitutive P_{EM7} promoter was constructed. The elements depicted are: Tn*7*-L and Tn*7*-R, left and right Tn*7* sites; T_0 and T_1, transcriptional terminators; Gm^R, gentamicin resistance gene; P_{EM7}, constitutive promoter; GFP, green fluorescent protein gene. A blue arrow represents the target region of recombineering oligonucleotides aimed to reconstruct the *gfp* ribosome-binding site (shown as a red square).

(B) Partial sequence of the four recombineering oligonucleotides (Table S1) designed to introduce SD motifs upstream of the *gfp* gene. RBS-C_6 and RBS-C_9 insert, respectively, the semi-canonical AGGAGG and the canonical TAAGGAGGT SD motifs eight nucleotides upstream the ATG start codon of the *gfp* (underlined); RBS-Deg_6 and RBS-Deg_9 insert, the randomized sequences RRRRRR and TARRRRRRT, where R stands for A (adenine) or G (guanine). Each degenerated oligonucleotide comprises a pool of 64 variants (2^6) with all possible combinations A/G.

(C) The mini-Tn*7* device was inserted in the *att*Tn*7* site of *P. putida* EM42. Upon transformation with pSEVA2314-*rec2-mutL*$_{E36K}^{PP}$, the resulting strain *P. putida* TA245 (pSEVA2314-*rec2-mutL*$_{E36K}^{PP}$) was subjected to one HEMSE cycle with the recombineering oligos in independent experiments. After plating in LB-GmKm-charcoal, GFP-positive clones were identified. A plate from the screening of RBS-Deg_9 is also shown, with a magnification of a fluorescent colony.

experiments with oligonucleotides designed for creating ribosomal binding site (RBSs) variants. The business parts of such oligonucleotides are shown in Figure 5B. As controls we used oligos named RBS-C_6 and RBS-C_9. These ssDNA enter, respectively, a short and an extended SD sequence, 8 bp upstream of the start codon of the *gfp* gene, using as a reference the *P. putida* 16S ribosomal gene and containing the core for optimal translation of 5′-GAGG-3′ (Shine and Dalgarno, 1975; Kozak, 1983; Farasat et al., 2014). For RBS diversification we used oligonucleotides RBS-Deg_6 and RBS-Deg_9 (Figure 5B), which include soft randomized sequences with discrete changes R (A or G) that cover six degenerated positions with a potential to generate 64 (= 2^6) combinations. This was expected to create a large population of RBS of different efficacies, which could be quantified through fluorescent emission of individual cells.

For the experiments described in the following discussion, *P. putida* TA245 (pSEVA2314-*rec2-mutL*$_{E36K}^{PP}$) was separately subject to one recombineering cycle with each of four oligos of Figure 5B, after which cells were diluted and plated in charcoal-LB agar for easing visual detection of colonies emitting low fluorescence on a black background. Positive controls RBS-C_6 and RBS-C_9 allowed the estimation of editing frequencies as GFP^+ cells/total number of cells, which resulted in 5.9×10^{-4} and 9.9×10^{-4}, respectively. Those values were relatively low when compared with the recombineering efficiencies reported earlier for single changes ($\sim 1 \times 10^{-2}$). This could be possibly due to the shorter homology arms of the oligos (30 nucleotides [nts]) and the extended sequence inserted between them (Aparicio et al., 2020). Yet, these figures provided a reference for subsequent quantification of the effect of soft-randomized oligos RBS-Deg_6 and RBS-Deg_9. After treatment with these, cultures were diluted and plated for inspection of ~9,000 colonies resulting of each recombineering experiment. Visual screening of the colonies revealed the appearance of 67 and 53 fluorescent clones coming, respectively, from experiments with RBS-Deg_6 and RBS-Deg_9. These 120 clones were picked up for further analysis. PCR and sequencing of the region upstream the *gfp* gene allowed identification of 14 variants of RBS-Deg_6 and 17 variants of RBS-Deg_9,

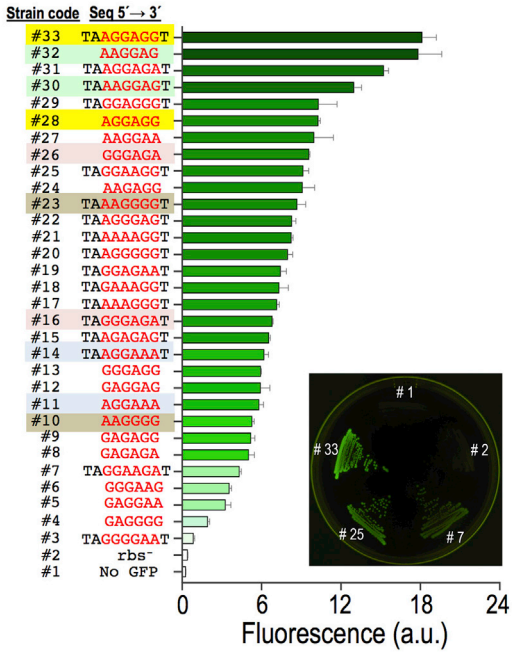

Figure 6. Characterization of the Diversified Library of SD Sequences

The screening of the HEMSE experiments performed in *P. putida* TA245 (pSEVA2314-*rec2-mutL*$_{E36K}^{PP}$) with RBS-Deg$_6$ and RBS-Deg$_9$ yielded 31 variants in the ribosome-binding site of the *gfp* gene. The GFP expression of this library was analyzed by flow cytometry including two negative controls: *P. putida* EM42 (Strain #1), in which there is no *gfp* gene, and the ancestral strain *P. putida* TA245 (pSEVA2314-*rec2-mutL*$_{E36K}^{PP}$), harboring the mini-Tn*7* and the *gfp* gene but lacking the original SD sequence (Strain #2). The plot shows the mean fluorescent emission of individual clones from two biological replicas with standard deviations. A Strain Code was assigned to each variant analyzed, and the putative SD sequence identified 8 nts upstream of the *gfp* start codon is shown. Variants showing identical sequence in the randomized region are highlighted with the same color. A plate of LB-charcoal agar with streaks of the two controls and three representative clones exhibiting low, medium, and high signal rates (#7, #25, and #33, respectively) is also depicted under UV light.

the GFP levels of which were measured by flow cytometry. The results plotted in Figure 6 show that the different variants delivered emissions ranging from very low to high fluorescent levels across a 20-fold change span. It is worth highlighting that the best RBS of the series (Strain Code #33, Figure 6) has a perfect match with the complementary sequence of the last 9 nts of the 16S ribosomal RNA of *P. putida* (PP_16SA). Other clones (e.g., #32; RBS = 5′-AAGGAG-3′) also displayed high fluorescence levels. Interestingly, a few productive variants contained the same 6-nt sequence in the degenerated region regardless of the type of randomized oligo (e.g., #32 = #30, #26 = #16, #14 = #11, and #23 = #10). Although most high-signal variants belong to the longer RBS-C$_9$-borne clones, a comparison of signals does not support the hypothesis that longer complementarity to the 16S ribosomal sequence correlates with more efficient translation. Other factors have been proposed to affect translation efficacy of RBS variants, such as the stability and secondary structure of RNA and transcriptional efficiency (Chen et al., 1994; Salis et al., 2009). Regardless of the possible biological significance of the results, the data of Figure 6 certifies the efficacy of the HEMSE platform to generate diversity in specific genomic segments—a welcome feature that can doubtless be multiplexed to other chromosomal locations as required.

DISCUSSION

In this work we have merged and adapted to *P. putida* and in a single platform three of the most efficacious genetic tools available to metabolic engineers for generating diversity *in vivo* focused on a predetermined number of chromosomal DNA segments: ssDNA recombineering (Wang et al., 2009), portable MAGE (Nyerges et al., 2016), and DIvERGE (Nyerges et al., 2018). Although conceptually identical to such methods already applied to *E. coli*, their recreation in a non-enterobacterial species involved (1) the search and testing of functional equivalents of the parts involved but recruited from *Pseudomonas* genomes and (2) adaptation and optimization to the distinct physiology of the species and strain at stake. Although we have not made a side-by-side comparison of the frequencies resulting from standard MAGE in *E. coli* and the ones presented in this work, numbers in the range of 10% replacements after 10 recombineering cycles could be sufficient to implement the same powerful method in *P. putida*. We are reluctant, however, to use the same acronym, because the automation feature is not in sight and the multiplexing is still problematic with the current efficiencies.

One can envision various ways through which HEMSE could be further improved. End-terminal degradation of the mutagenic oligos *in vivo* does not seem to be an issue: performance of 5′-phosphorothioated ssDNA (which cannot be degraded by exonucleases, Wang et al., 2009) is indistinguishable from non-phosphorothioated equivalents (Aparicio et al., 2020). However, the nature and origin of the recombinase

that catalyzes invasion of the DNA replication fork by the synthetic oligo makes a considerable difference (Chang et al., 2019). It is possible that such recombinases act in concert with additional endogenous proteins that could be characteristic of each species (Caldwell et al., 2019; Yin et al., 2019). It seems thus desirable that future alternatives to the Rec2 activity encoded in pSEVA2314-*rec2-mutL*$_{E36K}^{PP}$ (Figure 1) are mined in species-specific *Pseudomonas* genomes and phages—by themselves or in combination with other complementary genes. It should be straightforward to then replace the *rec2* of pSEVA2314-*rec2-mutL*$_{E36K}^{PP}$ by the improved counterparts, should they appear (e.g., Wannier et al., 2020), while maintaining the rest of the hereby described HEMSE protocol.

Limitations of the Study

As stated, one key bottleneck for implementing ssDNA recombineering in non-enteric bacteria is the efficacy of the core recombinase adopted in the experimental workflow. The work presented in this article is based on the one named Rec2, which emerged as the best in a limited bioinformatic and wet survey of ssDNA-binding proteins able to promote ssDNA invasion of the chromosomal replication fork (Ricaurte et al., 2018). However, it is most likely that other recombinases, whether naturally occurring or purposely engineered, may work better and could easily replace the Rec2 variant in our genome-editing pipeline whenever available. A second limitation is the somewhat poor ability of *P. putida* to capture exogenously added DNA, let alone ssDNA, as required for the hereby described method. Any progress in making this species—or any other—a better recipient of synthetic DNA will instantly translate in improved recombineering frequencies. Finally, the whole experimental workflow for multiple-site ssDNA recombineering is thus far restricted to manual implementation of the corresponding cycles. Despite the potential for automation claimed in the earliest description of MAGE (Wang et al., 2009), the cell separation step necessary for transforming bacteria with the mutagenic oligonucleotides still remains as a technical bottleneck that needs to be satisfactorily solved.

METHODS

All methods can be found in the accompanying Transparent Methods supplemental file.

SUPPLEMENTAL INFORMATION

Supplemental Information can be found online at https://doi.org/10.1016/j.isci.2020.100946.

ACKNOWLEDGMENTS

The authors are indebted to Sebastian S. Cocioba for posting in Twitter the useful recipe of LB-charcoal medium (https://twitter.com/ATinyGreenCell/status/1037332606432555009) and to Csaba Pal (Institute of Biochemistry, Biological Research Center, Szeged) for his continued support. This work was funded by the MADONNA (H2020-FET-OPEN-RIA-2017-1-766975), BioRoboost (H2020-NMBP-BIO-CSA-2018), SYNBIO4FLAV (H2020-NMBP/0500), and MIX-UP (H2020-Grant 870294) contracts of the European Union and the S2017/BMD-3691 InGEMICS-CM Project of the Comunidad de Madrid (European Structural and Investment Funds).

AUTHOR CONTRIBUTIONS

T.A., E.M.-G., A.N., and V.d.L. designed the study. T.A. performed the experiments. T.A., E.M.-G., and V.d.L. wrote the manuscript.

DECLARATION OF INTERESTS

Authors declare no conflict of interest.

Received: November 21, 2019
Revised: February 6, 2020
Accepted: February 21, 2020
Published: March 27, 2020

REFERENCES

Aparicio, T., Jensen, S.I., Nielsen, A.T., de Lorenzo, V., and Martinez-Garcia, E. (2016). The Ssr protein (T1E_1405) from *Pseudomonas putida* DOT-T1E enables oligonucleotide-based recombineering in platform strain *P. putida* EM42. Biotechnol. J. *11*, 1309–1319.

Aparicio, T., de Lorenzo, V., and Martinez-Garcia, E. (2019a). Improved thermotolerance of genome-reduced *Pseudomonas putida* EM42 enables effective functioning of the P_L/cI857 system. Biotechnol. J. *14*, e1800483.

Aparicio, T., de Lorenzo, V., and Martínez-García, E. (2020). A broad host range plasmid-based roadmap for ssDNA-based recombineering in gram-negative bacteria. In Horizontal Gene Transfer: Methods and Protocols, F. de la Cruz, ed. (Springer US), pp. 383–398.

Aparicio, T., Nyerges, A., Nagy, I., Pal, C., Martinez-Garcia, E., and de Lorenzo, V. (2019). Mismatch repair hierarchy of *Pseudomonas putida* revealed by mutagenic ssDNA recombineering of the *pyrF* gene. Environ. Microbiol. *22*, 45–58.

Bao, Z., Cartinhour, S., and Swingle, B. (2012). Substrate and target sequence length influence RecTE(P_{syr}) recombineering efficiency in *Pseudomonas syringae*. PLoS One *7*, e50617.

Caldwell, B.J., Zakharova, E., Filsinger, G.T., Wannier, T.M., Hempfling, J.P., Chun-Der, L., Pei, D., Church, G.M., and Bell, C.E. (2019). Crystal structure of the Redbeta C-terminal domain in complex with lambda Exonuclease reveals an unexpected homology with lambda Orf and an interaction with *Escherichia coli* single stranded DNA binding protein. Nucleic Acids Res. *47*, 1950–1963.

Carr, P.A., Wang, H.H., Sterling, B., Isaacs, F.J., Lajoie, M.J., Xu, G., Church, G.M., and Jacobson, J.M. (2012). Enhanced multiplex genome engineering through co-operative oligonucleotide co-selection. Nucleic Acids Res. *40*, e132.

Chang, Y., Wang, Q., Su, T., and Qi, Q. (2019). The efficiency for recombineering is dependent on the source of the phage recombinase function unit. bioRxiv, 745448, https://doi.org/10.1101/745448.

Chen, H., Bjerknes, M., Kumar, R., and Jay, E. (1994). Determination of the optimal aligned spacing between the Shine-Dalgarno sequence and the translation initiation codon of *Escherichia coli* mRNAs. Nucleic Acids Res. *22*, 4953–4957.

Chen, W., Zhang, Y., Zhang, Y., Pi, Y., Gu, T., Song, L., Wang, Y., and Ji, Q. (2018). CRISPR/Cas9-based genome editing in *Pseudomonas aeruginosa* and cytidine deaminase-mediated base editing in *Pseudomonas* species. iScience *6*, 222–231.

Costantino, N., and Court, D.L. (2003). Enhanced levels of lambda Red-mediated recombinants in mismatch repair mutants. Proc. Natl. Acad. Sci. U S A *100*, 15748–15753.

Datsenko, K.A., and Wanner, B.L. (2000). One-step inactivation of chromosomal genes in *Escherichia coli* K-12 using PCR products. Proc. Natl. Acad. Sci. U S A *97*, 6640–6645.

Ellis, H.M., Yu, D., DiTizio, T., and Court, D.L. (2001). High efficiency mutagenesis, repair, and engineering of chromosomal DNA using single-stranded oligonucleotides. Proc. Natl. Acad. Sci. U S A *98*, 6742–6746.

Farasat, I., Kushwaha, M., Collens, J., Easterbrook, M., Guido, M., and Salis, H.M. (2014). Efficient search, mapping, and optimization of multi-protein genetic systems in diverse bacteria. Mol. Syst. Biol. *10*, 731.

Gallagher, R.R., Li, Z., Lewis, A.O., and Isaacs, F.J. (2014). Rapid editing and evolution of bacterial genomes using libraries of synthetic DNA. Nat. Protoc. *9*, 2301–2316.

Hueso-Gil, A., Nyerges, Á., Pál, C., Calles, B., and de Lorenzo, V. (2020). Multiple-site diversification of regulatory sequences enables inter-species operability of genetic devices. ACS Synth. Biol. *9*, 104–114.

Isaacs, F.J., Carr, P.A., Wang, H.H., Lajoie, M.J., Sterling, B., Kraal, L., Tolonen, A.C., Gianoulis, T.A., Goodman, D.B., Reppas, N.B., et al. (2011). Precise manipulation of chromosomes in vivo enables genome-wide codon replacement. Science *333*, 348–353.

Jiang, W., Bikard, D., Cox, D., Zhang, F., and Marraffini, L.A. (2013). RNA-guided editing of bacterial genomes using CRISPR-Cas systems. Nat. Biotechnol. *31*, 233–239.

Kozak, M. (1983). Comparison of initiation of protein synthesis in procaryotes, eucaryotes, and organelles. Microbiol. Rev. *47*, 1–45.

Lesic, B., and Rahme, L.G. (2008). Use of the lambda Red recombinase system to rapidly generate mutants in *Pseudomonas aeruginosa*. BMC Mol. Biol. *9*, 20.

Liang, R., and Liu, J. (2010). Scarless and sequential gene modification in *Pseudomonas* using PCR product flanked by short homology regions. BMC Microbiol. *10*, 209.

Lopes, A., Amarir-Bouhram, J., Faure, G., Petit, M.-A., and Guerois, R. (2010). Detection of novel recombinases in bacteriophage genomes unveils Rad52, Rad51 and Gp2. 5 remote homologs. Nucleic Acids Res. *38*, 3952–3962.

Luo, X., Yang, Y., Ling, W., Zhuang, H., Li, Q., and Shang, G. (2016). *Pseudomonas putida* KT2440 markerless gene deletion using a combination of lambda Red recombineering and Cre/loxP site-specific recombination. FEMS Microbiol. Lett. *363*, fnw014.

Martínez-García, E., and de Lorenzo, V. (2019). *Pseudomonas putida* in the quest of programmable chemistry. Curr. Opin. Biotechnol. *59*, 111–121.

Martínez-García, E., Nikel, P.I., Aparicio, T., and de Lorenzo, V. (2014). Pseudomonas 2.0: genetic upgrading of *P. putida* KT2440 as an enhanced host for heterologous gene expression. Microb. Cell Fact. *13*, 159.

Nikel, P.I., Martinez-Garcia, E., and De Lorenzo, V. (2014). Biotechnological domestication of pseudomonads using synthetic biology. Nat. Rev. Microbiol. *12*, 368–379.

Nikel, P.I., Chavarria, M., Danchin, A., and de Lorenzo, V. (2016). From dirt to industrial applications: *Pseudomonas putida* as a synthetic biology chassis for hosting harsh biochemical reactions. Curr. Opin. Chem. Biol. *34*, 20–29.

Nyerges, A., Csorgo, B., Nagy, I., Latinovics, D., Szamecz, B., Posfai, G., and Pal, C. (2014). Conditional DNA repair mutants enable highly precise genome engineering. Nucleic Acids Res. *42*, e62.

Nyerges, A., Csorgo, B., Nagy, I., Balint, B., Bihari, P., Lazar, V., Apjok, G., Umenhoffer, K., Bogos, B., Pósfai, G., et al. (2016). A highly precise and portable genome engineering method allows comparison of mutational effects across bacterial species. Proc. Natl. Acad. Sci. U S A *113*, 2502–2507.

Nyerges, A., Csorgo, B., Draskovits, G., Kintses, B., Szili, P., Ferenc, G., Révész, T., Ari, E., Nagy, I., Bálint, B., et al. (2018). Directed evolution of multiple genomic loci allows the prediction of antibiotic resistance. Proc. Natl. Acad. Sci. U S A *115*, E5726–E5735.

Oesterle, S., Wuethrich, I., and Panke, S. (2017). Toward genome-based metabolic engineering in bacteria. Adv. Appl. Microbiol. *101*, 49–82.

Ostrov, N., Landon, M., Guell, M., Kuznetsov, G., Teramoto, J., Cervantes, N., Zhou, M., Singh, K., Napolitano, M.G., Moosburner, M., et al. (2016). Design, synthesis, and testing toward a 57-codon genome. Science *353*, 819–822.

Ricaurte, D.E., Martinez-Garcia, E., Nyerges, A., Pal, C., de Lorenzo, V., and Aparicio, T. (2018). A standardized workflow for surveying recombinases expands bacterial genome-editing capabilities. Microb. Biotechnol. *11*, 176–188.

Ronda, C., Pedersen, L.E., Sommer, M.O., and Nielsen, A.T. (2016). CRMAGE: CRISPR optimized mage recombineering. Sci. Rep. *6*, 19452.

Salis, H.M., Mirsky, E.A., and Voigt, C.A. (2009). Automated design of synthetic ribosome binding sites to control protein expression. Nat. Biotechnol. *27*, 946–950.

Shine, J., and Dalgarno, L. (1975). Determinant of cistron specificity in bacterial ribosomes. Nature *254*, 34–38.

Swingle, B., Bao, Z., Markel, E., Chambers, A., and Cartinhour, S. (2010a). Recombineering using RecTE from *Pseudomonas syringae*. Appl. Environ. Microbiol. *76*, 4960–4968.

Swingle, B., Markel, E., Costantino, N., Bubunenko, M.G., Cartinhour, S., and Court, D.L. (2010b). Oligonucleotide recombination in Gram-negative bacteria. Mol. Microbiol. *75*, 138–148.

Szili, P., Draskovits, G., Révész, T., Bogar, F., Balogh, D., Martinek, T., Daruka, L., Spohn, R.,

Vásárhelyi, B.M., Czikkely, M., et al. (2019). Rapid evolution of reduced susceptibility against a balanced dual-targeting antibiotic through stepping-stone mutations. Antimicrob. Agents Chemother. *63*, e00207–e00219.

van Pijkeren, J.-P., Neoh, K.M., Sirias, D., Findley, A.S., and Britton, R.A. (2012). Exploring optimization parameters to increase ssDNA recombineering in *Lactococcus lactis* and *Lactobacillus reuteri*. Bioengineered *3*, 209–217.

Wang, H.H., Isaacs, F.J., Carr, P.A., Sun, Z.Z., Xu, G., Forest, C.R., and Church, G.M. (2009). Programming cells by multiplex genome engineering and accelerated evolution. Nature *460*, 894–898.

Wannier, T.M., Nyerges, A., Kuchwara, H.M., Czikkely, M., Balogh, D., Filsinger, G.T., Borders, N.C., Gregg, C.J., Lajoie, M.J., Rios, X., et al. (2020). Improved bacterial recombineering by parallelized protein discovery. bioRxiv. https://doi.org/10.1101/2020.01.14.906594.

Yin, J., Zheng, W., Gao, Y., Jiang, C., Shi, H., Diao, X., Li, S., Chen, H., Wang, H., Li, R., et al. (2019). Single-stranded DNA-binding protein and exogenous RecBCD inhibitors enhance phage-derived homologous recombination in *Pseudomonas*. iScience *14*, 1–14.

Yu, D., Ellis, H.M., Lee, E.C., Jenkins, N.A., Copeland, N.G., and Court, D.L. (2000). An efficient recombination system for chromosome engineering in *Escherichia coli*. Proc. Natl. Acad. Sci. U S A *97*, 5978–5983.

iScience, Volume *23*

Supplemental Information

High-Efficiency Multi-site Genomic Editing of *Pseudomonas putida* through Thermoinducible ssDNA Recombineering

Tomas Aparicio, Akos Nyerges, Esteban Martínez-García, and Víctor de Lorenzo

SUPPLEMENTARY INFORMATION

TRANSPARENT METHODS

Strains and media

The bacterial strains employed in this study are listed in Supplementary Table S2. *E. coli* and *P. putida* strains were grown in liquid LB with shaking (170 rpm) at 37 ºC and 30 ºC, respectively (Sambrook et al., 1989) with the exception of *E. coli* strains bearing SEVA plasmids endowed with the P_L/cI857 thermo-inducible expression system (cargo #14; i.e. pSEVA2514-*rec2-mutL*$_{E36K}^{PP}$ and derivatives), which were grown at 30 ºC to avoid promoter activation. After electroporation, recovery during recombineering experiments was performed in Terrific Broth without glycerol (TB: 12 g L^{-1} tryptone, 24 g L^{-1} yeast extract, 2 g L^{-1} KH_2PO_4, 9.4 g L^{-1} K_2HPO_4). M9 minimal media was prepared according to (Sambrook et al., 1989). Solid media was prepared adding 15 g L^{-1} of agar to liquid media. M9 solid media was supplemented with 0.2% (w/v) citrate and appropriate antibiotics to select *P. putida* cells in mating experiments. Liquid and solid media were added, when necessary, with 50 µg ml^{-1} of kanamycin (Km), 15 µg ml^{-1} of gentamicin (Gm) for *P. putida* and 10 µg ml^{-1} of the same antibiotic for *E. coli*, 30 µg ml^{-1} of chloramphenicol (Cm), 100 µg ml^{-1} of streptomycin (Sm), 100 µg ml^{-1} of rifampicin (Rif), 50 µg ml^{-1} of nalidixic acid (Nal), 20 µg ml^{-1} of Uracil (Ura), 250 µg ml^{-1} of 5-fluoroorotic acid (5-FOA) and 5 mM of benzoic acid (pH 11). For screening of fluorescent colonies, LB solid media was prepared with 1 mg ml^{-1} of activated charcoal (Sigma-Aldrich Ref. C9157-500G) in order to better discriminate low-signal colonies. Activated charcoal was added to the LB-Agar prior autoclaving and the media poured into 150 mm Petri dishes after vigorous shaking to evenly distribute the insoluble charcoal particles.

General procedures, primers and bacterial transformation

Standard DNA manipulations were carried out following routine protocols (Sambrook et al., 1989) and according to manufacturer recommendations. Isothermal Assembly was performed with Gibson Assembly® Master Mix (New England Biolabs, Ipswich, MA, USA). Plasmidic DNA was

purified with the QIAprep® Spin Miniprep Kit, both purchased from Qiagen (Valencia, CA, USA). DNA Amplitools Master Mix (Biotools, Madrid, Spain) was used for diagnosis PCRs and amplification of DNA fragments for cloning purposes was done with Q5 polymerase (New England Biolabs, Ipswich, MA, USA). Synthetic oligonucleotides used in this study are listed in Supplementary Table S1 and were purchased from Sigma-Aldrich (St. Louis, MO, USA). PCR products were purified with the Nucleospin® Gel and PCR Clean-up Kit (Macherey-Nagel, Düren, Germany). DNA sequencing was performed in Macrogen (Spain). Transformation of *E. coli* strains was carried out with chemically competent cells using the $CaCl_2$ method (Sambrook et al., 1989). Plasmids were introduced in *P. putida* strains via tripartite mating as described in (Martinez-Garcia and de Lorenzo, 2012) and selected in solid M9 minimal media supplemented with 0.2% w/v citrate and appropriate antibiotics. Tetra-parental mating was used as described by (Choi et al., 2005) to insert the mini-transposon Tn*7*-M-P_{EM7}-*gfp* -RBS^{-} into the *att*Tn*7* site of *P. putida* EM42, using M9-citrate-Gm as selective media (see below for details).

Construction of plasmids and strains.

The medium-high copy number plasmid pSEVA2514-*rec2*-*mutL*$_{E36K}^{PP}$ (Supplementary Table S2) was used for the construction of two derivatives bearing low- and medium- copy number origins of replication. This plasmid was cut with PacI/SpeI and the 4.2 Kb DNA band, containing the *rec2* and *mutL*$_{E36K}^{PP}$ genes under the control of the thermo-inducible system P_L/*c*I857, was ligated to PacI/SpeI restricted plasmids pSEVA221 (low copy number) and pSEVA231 (medium copy number). Ligations were transformed into *E. coli* CC118 and selection was made in LB-Km plates, obtaining plasmids pSEVA2214-*rec2*-*mutL*$_{E36K}^{PP}$ and pSEVA2314-*rec2*-*mutL*$_{E36K}^{PP}$. Both constructs were separately introduced in *P. putida* EM42 by tri-parental matings followed by selection in M9-citrate-Km solid media, obtaining the strains *P. putida* EM42 (pSEVA2214-*rec2*-*mutL*$_{E36K}^{PP}$) and *P. putida* EM42 (pSEVA2314-*rec2*-*mutL*$_{E36K}^{PP}$). *P. putida* EM42 was also transformed by the same method with pSEVA2314, generating the control strain *P. putida* EM42 (pSEVA2314). A Tn*7* mini-transposon with the *gfp* gene under the control of the constitutive P_{EM7} promoter, but lacking the ribosome binding site (RBS) sequence, was constructed. To this end, first the *gfp* gene was placed under the control of the P_{EM7} promoter: plasmid pSEVA637 (Supplementary Table S2) was cut with HindIII/SpeI and the purified 0.7 Kb band (RBS + *gfp*

gene) was ligated to the pSEVA237R-PEM7 (Supplementary Table S2) backbone digested with HindIII/SpeI. Upon transformation in *E. coli* CC118 and selection on LB-Km plates, the resulting plasmid (pSEVA237-PEM7) was digested with PacI/SpeI and the purified 0.9 Kb band (containing the *gfp* gene under the control of the P_{EM7} and bearing a consensus 5´-AGGAGG-3´ RBS sequence) was ligated to a pTn7-M plasmid restricted with the same enzymes. Ligation mixture was used to transform *E. coli* competent cells and selection was done in LB-KmGm plates. The resulting plasmid, pTn7-M-PEM7-GFP, was used as a template to eliminate the RBS sequence. In order to achieve this, the plasmid was PCR amplified with primers Tn7-PEM7-F/ Tn7-PEM7-R (Tm= 58 ºC, 2 min. elongation, Q5 polymerase). The primers were designed to i) amplify the whole plasmid with the exception of the 7-nt Shine Dalgarno motif 5´-AGGAGGA-3´ located 7-nt away from the *gfp* start codon, ii) generate an PCR product sharing a 40-bp sequence at both sides of the molecule to allow isothermal assembly of the amplicon. The 3.9 Kb PCR product was purified and subjected to Gibson Assembly and the reaction was transformed into *E. coli*. Selection was made in LB-KmGm plates, thus obtaining the plasmid pTn7-M-PEM7-GFP-RBS^{-}. The region between the P_{EM7} promoter and the end of the *gfp* gene was fully sequenced with primers PS2 and PEM7-F to ensure the correct deletion of the RBS sequence. *E. coli* (pTn7-M-PEM7-GFP-RBS^{-}) was used as the donor strain to introduce the mini-transposon in the *att*Tn7 site of *P. putida* EM42. Both strains and the helper strains *E. coli* HB101 (pRK600) and *E. coli* (pTNS2) were used in a tetra-parental mating followed by selection in M9-citrate-Gm solid media. Colonies were streaked in the same media and subjected to two diagnostic PCRs to check the mini-transposon insertion. PCRs with primer pairs PS2/ PP5408-F (Tm= 60 ºC, 1 min. 30 seconds elongation) and PEM7-F/Tn7-GlmS (Tm= 60 ºC, 1 min. elongation) yielded bands of 2.2 Kb and 1.2 Kb, respectively, confirming the correct integration of the transposon in the *att*Tn7 locus. The resulting strain *P. putida* EM42::Tn7-M-P_{EM7}-*gfp*-RBS^{-} (referred as *P. putida* TA245 in Supplementary Table S2) was transformed by tripartite mating with pSEVA2314-*rec2*-*mutL*$_{E36K}^{PP}$ plasmid. After selection on M9-citrate-KmGm plates, the strain *P. putida* TA245 (pSEVA2314-*rec2*-*mutL*$_{E36K}^{PP}$) was obtained. Integrity of the constructs described above, either in *E. coli* or *P. putida*, was always checked by miniprep, restriction and agarose gel visualization.

Oligonucleotide design, recombineering protocol, cycling procedure and screening

The nine oligonucleotides used in this work for recombineering experiments (SR, NR, RR, PR, CR, RBS-C_6, RBS-Deg_6, RBS-C_9, RBS-Deg_9) were designed to introduce different allelic changes targeting the lagging strand of the *P. putida* chromosome. Supplementary Table S3 summarizes the main features of each oligonucleotide while complete sequence and additional details can be found in Supplementary Table S1. The recombineering protocol used here relies in the co-expression of the Rec2 recombinase and the $MutL_{E36K}^{PP}$ dominant negative allele from plasmids endowed with the thermo-inducible P_L/*c*I857 expression system (pSEVA2214-*rec2-mutL*$_{E36K}^{PP}$, pSEVA2314-*rec2-mutL*$_{E36K}^{PP}$ or pSEVA2514-*rec2-mutL*$_{E36K}^{PP}$). The protocol is basically identical to that described previously in (Aparicio et al., 2019b). Overnight cultures of *P. putida* strains harboring the proper plasmid were used to inoculate 20 ml of fresh LB-Km at OD_{600} = 0.1 in 100 ml Erlenmeyer flasks. Cultures were incubated at 30 ºC with vigorous shaking (170 rpm) until OD_{600} ~ 1.0 and flasks were then placed in a water bath at 42 ºC for 5 minutes to increase rapidly the temperature and induce the P_L promoter. Ten additional minutes of incubation at 42 ºC was performed in an air shaker at 250 rpm (induction total time at 42 ºC= 15 minutes) to trigger the expression of *rec2-mutL*$_{E36K}^{PP}$ genes, followed by 5 minutes in ice to cool down the bacterial culture and stop the induction. In non-induced cultures the heat-shock and cooling down steps were not performed. Competent cells were then prepared transferring 10 ml of each culture to 50-ml conical tubes and centrifuging the cells at 3,220 g/ 5 minutes. Cell pellets were resuspended in 10 ml of 300 mM sucrose and washed two additional times with 5 and 1 ml of the same solution. After centrifugation in a bench-top centrifuge (10,000 rpm, 1 minute), cellular pellets were finally resuspended in 200 μl of 300 mM sucrose and 100 μl of this suspension was added with the recombineering oligonucleotide. For single-oligonucleotide experiments, 1 μl from a 100 μM stock was used (1 μM final concentration). For multiplexed experiments, 10 μl of each oligonucleotide stock at 100 μM (SR, NR, RR, PR and CR) were mixed and 3 μl of this mixture were added to the competent cells (accounting for 0.6 μM of each oligo.). The cell suspension was mixed thoroughly by pipetting, placed in an electroporation cuvette (Bio-Rad, 2 mm-gap width) and electroporated at 2.5 kV in a Micropulser™ device (Bio-Rad Laboratories, Hercules, CA, USA). Cells were immediately inoculated in 5 ml of fresh TB in 100 ml Erlenmeyer flaks and recovered at 30 ºC/ 170 rpm. Before plating the cells for screening of allelic replacements, different recovery times and TB additions were used depending on the experiment. For one cycle recombineering experiments, overnight recovery was done in TB for assays with SR and NR

oligonucleotides while for experiments with oligonucleotides RBS-C_6, RBS-Deg_6, RBS-C_9 and RBS-Deg_9, TB supplemented with Km and Gm was preferred. Specifications for cycled recombineering assays (HEMSE) are depicted below.

High-efficiency multi-site genomic editing protocol

HEMSE is a cycled recombineering protocol run in a multiplexed fashion. The procedure involves a standard recombineering protocol in which, as explained before, cultures were subjected to electrotransformation with an equimolar mixture of several oligonucleotides. The recovery was performed in TB added with Km in order to maintain the plasmid along the cycles, and the incubation proceeded at 30 ºC with vigorous shaking (170 rpm) until an OD_{600} ~ 1.0 (Cycle-I). Culture aliquots were withdrawn for screening and the bacterial culture entered in the next round of recombineering by performing induction at 42 ºC/ 15 minutes, competent cell preparation, oligonucleotide mixture electroporation and recovery till reaching again a cell density around 1.0 at 600 nm (Cycle-II). Further cycles proceeded in the same way (Fig. 3 of main text). Each cycle took one day in average and recovery, when necessary, was performed overnight at room temperature without shaking to avoid culture overgrowth. When recovery step was completed at the end of the day, cultures were stored at 4 ºC overnight. A new cycle was started in the next morning incubating the culture 30 minutes at 30 ºC (170 rpm) before the induction step. Screening of allelic changes after recombineering was performed plating aliquots of recovered cultures in the appropriate selective and/or non-selective solid media, as follows:

• In single-olignucleotide experiments with SR and NR oligonucleotides (one cycle), overnight cultures were plated in LB-Sm (dilutions 10^{-4} and 10^{-5} for induced cultures and 10^{-2} and 10^{-3} for non-induced bacteria) and LB-Nal (dilutions 10^{-4} and 10^{-5} for induced cultures and 10^{-2} and 10^{-3} for non-induced bacteria), respectively, to estimate the allelic replacements, while dilutions 10^{-7} and 10^{-8} were done in LB without antibiotics to count viable cells. Plates were incubated 18 h. at 30 ºC and CFUs annotated.

• In single-oligonucleotide experiments with RBS-C_6, RBS-Deg_6, RBS-C_9, RBS-Deg_9 oligos (one cycle), cultures recovered overnight were plated on 150 mm width LB-KmGm-activated charcoal

plates using 10^{-6} dilutions. This allowed an average of 500 colonies per plate. To facilitate the identification of colonies displaying low levels of fluorescence, plates were incubated at 30 ºC for 5 days. Fluorescent colonies were streaked in the same media and insertion of putative ribosome binding sites upstream the *gfp* gene were checked by PCR amplifying this DNA region with primers PS2/ PP5408-F (Tm= 60 ºC, 1 min. 30 seconds elongation, 1.0 Kb product) and sequencing the amplicon with primer ME-I-Gm-ExtR. Non-redundant clones with different sequences inserted were selected and glycerol stocks made prior characterization by flow cytometry.

• Allelic replacements in HEMSE experiments were screened after recovery steps (OD_{600} ~ 1.0) of cycle-I, cycle-V and cycle-X. Viable cells were estimated plating dilutions 10^{-7} and 10^{-8} in LB plates. Single mutants coming from SR-, NR-, RR- and PR-mediated recombineering were analyzed by plating dilutions 10^{-4} and 10^{-5} in LB-Sm, LB-Nal, LB-Rif and LB-5FOA-Ura plates. Plates were incubated 24 h at 30 ºC and total CFUs of single mutants (Sm^R, Nal^R, Rif^R and $5FOA^R$) and viable cells were taken. Twenty $5FOA^R$ colonies were replicated on M9-citrate and M9-citrate-5FOA-Ura plates in order to discriminate authentic *pyrF* mutants ($5FOA^R/Ura^-$) from spontaneous $5FOA^R$ mutants ($5FOA^R/Ura^+$), as stated in (Galvao and de Lorenzo, 2005; Aparicio et al., 2016). Colonies grown on both media were discounted of the total $5FOA^R$ numbers as *pyrF*-unrelated, spontaneous mutants. Dilutions 10^{-6} in LB-benzoate plates allowed the estimation of *catA*-I^- mutants simply by counting the dark-brown colonies appeared after 10 days of incubation at 30 ºC. *catA*-I^- mutants accumulate catechol, which turns into brown intermediates after spontaneous oxidation and polymerization (Jimenez et al., 2014). In previous assays aimed to obtain *catA*-I- mutants through recombineering with CR oligo, it was noticed that long incubations were necessary to appreciate the colored phenotype in solid media (Fig. S2). The observed dark-brown colonies were always *catA*-I^- mutants, as was demonstrated by amplification of *catA*-I gene (primers catA-F/catA-R, Tm 55 ºC, 1 minute elongation) and sequencing of the 0.5 Kb amplicon with primer catA-F (data not shown) in 20 selected colonies. Multiple gene editions were also analyzed plating cultures from cycles I, V and X on LB solid media supplemented either with Sm+Nal+ Rif+5FOA+Ura (four editions mediated by SR, NR, RR and PR oligonucleotides), 24 incubation at 30 ºC, or with Sm+Nal+Rif+5FOA+Ura+benzoate (five editions mediated by the 5 oligonucleotides used in this study), 10 days incubation at 30 ºC. For

this last experiment, there were considered quintuple mutants those colonies displaying resistance to Sm, Nal, Rif and 5FOA and also showing the characteristic brown phenotype of *catA*-I$^-$ mutants. The recombineering frequency (RF) was calculated as the ratio between the number of colonies showing a given phenotype and the number of viable cells within the experiment, being this ratio normalized to 10^9 viable cells for graphic representation.

In order to check the accuracy of the allelic replacements, 18 colonies showing the quintuple mutant phenotype (Sm^R, Nal^R, Rif^R, 5FOA^R and catechol accumulation) were checked by PCR amplification and sequencing of the target genes. For each bacterial clone, five different PCRs were set up to amplify: *rpsL* (primers rpsL-Fw/ rpsL-Rv, Tm 57 ºC, 45 seconds elongation, 0.8 Kb product), *gyrA* (primers gyrA-Fw/ gyrA-Rv, Tm 57 ºC, 45 seconds elongation, 0.4 Kb product), *rpoB* (primers rpoB-F/rpoB-R, Tm 57 ºC, 45 seconds elongation, 0.4 Kb product), *pyrF* (primers pyrF-F/pyrF-R, Tm 52 ºC, 1 minute elongation, 1.2 Kb product) and *catA-I* (primers catA-F/catA-R, Tm 55 ºC, 1 minute elongation, 0.5 Kb product). The purified PCR products were sequenced with the putative forward primers and the sequence analysed for the expected changes mediated by recombineering. All clones analysed (n=18; 100%) showed the correct changes, demonstrating that the observed phenotypes corresponded to mutations mediated by the HEMSE procedure. Single allelic replacements in HEMSE experiments were not confirmed by PCR and sequencing since previous works showed that virtually 100% of Sm^R, Nal^R and *pyrF*$^-$ mutants obtained by recombineering with oligos SR, NR and LM (almost identical to RR oligo used in this work) harbored the expected changes in the target genes *rpsL*, *gyrA* and *pyrF* (Ricaurte et al., 2018; Aparicio et al., 2019a). Preliminary studies in this work showed, on the other hand, that single Rif^R mutants also displayed 100% accuracy in the expected mutations of the target gene *rpoB* (data not shown). As explained before, *catA*-I$^-$, dark-brown colonies were also analyzed by PCR and sequencing in previous test experiments (data not shown), with analogous results.

Flow cytometry

The visual selection of fluorescent colonies from recombineering experiments with oligos RBS-Deg$_6$ and RBS-Deg$_9$ gave rise to a collection of 31 RBS insertion mutants showing a wide variety of fluorescent signals. Together with the negative controls of *P. putida* TA245 (insertion of Tn*7*-M-

P_{EM7}-*gfp*-RBS^{-}) and *P. putida* EM42 (no *gfp* gene), a total of 33 strains were characterized for GFP production. Each strain was inoculated from glycerol stocks in 2 ml of LB-KmGm (*P. putida* EM42 in LB; *P. putida* TA245 in LB-Gm) and cultured at 30 ºC/ 170 rpm. 0.5 ml of overnight cultures (OD_{600} ~ 2-3) were centrifuged and resuspended in 1 ml of filtered Phosphate Buffered Saline (PBS) 1X (8 mM Na_2HPO_4, 1.5mM KH_2PO_4, 3 mM KCl, 137 mM NaCl, pH.7.0). Fifty μl of each suspension was added to 450 μl of PBS 1X to obtain cellular samples with OD_{600} ~ 0.1-0.15. Samples were analyzed in a MACSQuant^{TM} VYB cytometer (Miltenyi Biotec, Bergisch Gladbach, Germany) to quantify the emission of fluorescence as indicated in (Martinez-Garcia et al., 2014). GFP was excited at 488 nm and the fluorescence signal was recovered with a 525±40 nm band-pass filter. For each sample, at least 100,000 events were analyzed and the FlowJo v. 9.6.2 software (FlowJo LLC, Ashland, OR, USA) was used to process the results. Population was gated to eliminate background noise and the median of the GFP-A channel of two biological replicas was used for graphical representation.

Data and Software Availability

GenBank accession numbers for the plasmids used in this study are the following:

pSEVA2214-*rec2*-*mutL*$_{E36K}^{PP}$ (MN688223)

pSEVA2314-*rec2*-*mutL*$_{E36K}^{PP}$ (MN688222)

pSEVA2514-*rec2*-*mutL*$_{E36K}^{PP}$ (MN180222)

SUPPLEMENTARY FIGURES

Figure S1. Rec2-independent editing in HEMSE assays (related to Fig. 4 of main text)

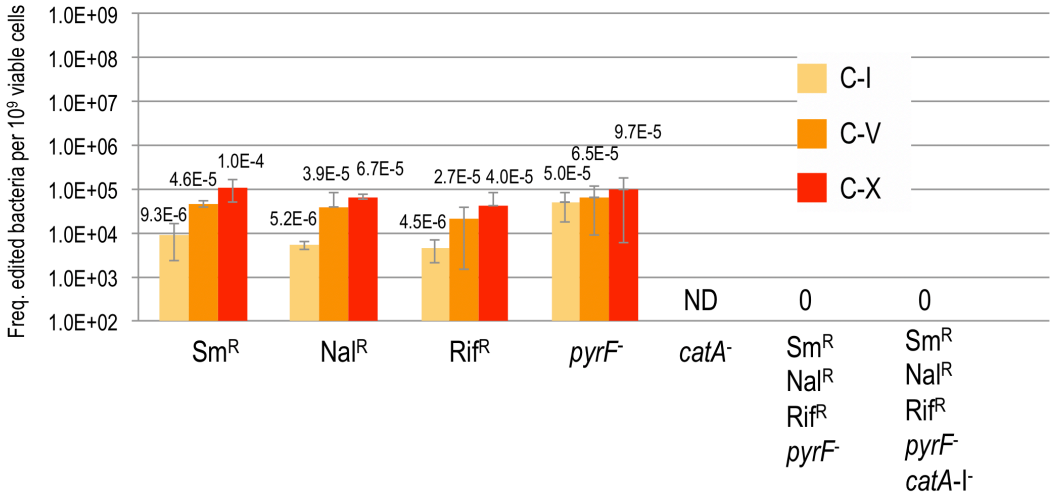

Editing efficiencies of single and multiple changes in the control strain *P. putida* EM42 harboring the empty plasmid pSEVA2314 were assayed applying 10 cycles of HEMSE and an equimolar mixture of oligos SR, NR, RR, PR and CR, following the same procedure explained in Figure 4A and 4B. See more details in Transparent Methods section. Allelic replacements of *catA*-I gene were not determined in these assays (ND), while multiple editions could not be detected (0).

Figure S2. Phenotype of *P. putida* EM42 *catA*-I$^-$ strain (related to Fig. 4 of main text).

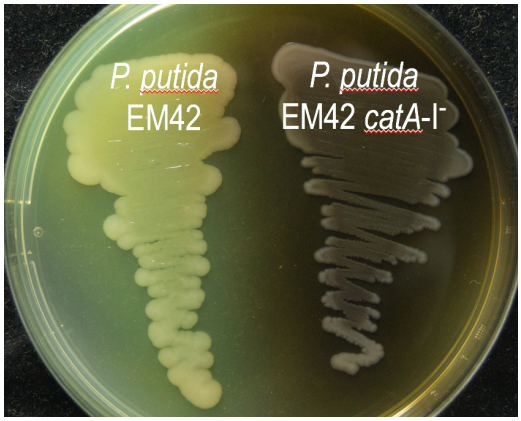

P. putida EM42 (pSEVA2314-*rec2*-*mutL*$_{E36K}^{PP}$) was subjected to recombineering with CR oligonucleotide (see Transparent Methods section). Three stop codons were inserted in the *catA*-I ORF, generating a mutant strain in which the metabolism of benzoic acid is impaired, leading to accumulation of catechol (Jimenez et al., 2014). Upon spontaneous oxidation and polymerization, catechol derivatives exhibit a characteristic dark-brown colour. *P. putida* EM42 and the *catA-I* mutant were grown in LB-Agar supplemented with benzoate 5 mM and incubated 10 days at 30 ºC to allow the visualization of the colored phenotype.

SUPPLEMENTARY TABLES

SUPPLEMENTARY TABLE S1. Oligonucleotides used in this study (related to Fig. 2 and Fig. 5 of main text).

Name	[(a)] Sequence (5' → 3')	Usage / Source
SR	G*T*C*A*GACGCACACGGCATACTTTACGCAG TGCCGAGTTAGGTTTT**G**TCGGCGTGGTGGTG TACACACGGGTGCACACGCCACGACGCTGC	Recombineering oligo for *rpsL* gene: AAA (K43) changed to ACA (T43), mismatch A:G, confers Sm resistance (Ricaurte et al., 2018)
rpsL-Fw	GACATGAAATGTTGCCGATG	To amplify and sequence part of *rpsL* gene of *P. putida* /(Ricaurte et al., 2018)
rpsL-Rv	CTGTTCTTGCGTGCTTTGAC	With rpsL-Fw, to amplify part of *rpsL* gene of *P. putida* (Ricaurte et al., 2018)
NR	AACGAGAACGGCTGGGCCATACGCACGATGG T**A**TT**T**GTAGACCGCAGTGTCGCCGTGCGGGTG GTA	Recombineering oligo for *gyrA* gene: GAC (D87) changed to AAT (N87), mismatches G:T and C:A, confers Nal resistance (Aparicio et al., 2019b)
gyrA-F	GGCCAAAGAAATCCTCCCGGTCAA	To amplify and sequence part of *gyrA* gene of *P. putida* (Aparicio et al., 2019b)
gyrA-R	AGCAGGTTGGGAATACGCGTCG	To amplify and sequence part of *gyrA* gene of *P. putida* (Aparicio et al., 2019b)
RR	TCCGAGAGAGGGTTGTTCTGGTCCATGAAC**A** GGGACAGCTGGCTGGAACCGAAGAACTCT	Recombineering oligo for *rpoB* gene: CAG (Q518) changed to CTG (L518), mismatch A:A, confers Rif resistance. This work
rpoB-F	CCTGGGTAACCGTCGCGTACGGTG	To amplify and sequence part of *rpoB* gene of *P. putida.* This work
rpoB-R	CGCCTTCCTTCACCACGCGGTACG	To amplify and sequence part of *rpoB* gene of *P. putida.* This work
PR	AGGTCCAGGAACACTTCGAAGCCCTTGTCACA CAGGGTTT**A**GACAATGCCCGAAGCGCTGCTG	Recombineering oligo for *pyrF* gene: GAA (E50) changed to TAA

	GTGAACAGCTCCTTGCCA	(Stop), mismatch A:G, confers 5FOA resistance and uracil auxotrophy. This work
pyrF-F	CGAGGGCTATGATGAGTATC	To amplify and sequence the *pyrF* gene of *P. putida* (Aparicio et al., 2016)
pyrF-R	GTCAGGTGAAGAGCAAAGAG	To amplify and sequence the *pyrF* gene of *P. putida* (Aparicio et al., 2016)
CR	GCAGCACGCGCAGAATGATCTGCTTGAAGCG CGGGTTTCCCTATTATCATTCGGCATGGTCCA GGCCAGCTACCCGGTTGAAGAAGGCT	Recombineering oligo for *catA-I* gene: insertion of three stop codons truncates the ORF, giving rise to brown colonies in presence of benzoate. This work
catA-F	AACTCGTCCTCGGTAATCTC	To amplify and sequence part of *catA-I* gene of *P. putida.* This work
catA-R	CAGCAATCAAGGAGATAACC	To amplify and sequence part of *catA-I* gene of *P. putida.* This work
Tn7-PEM7-F	AAAACATATGAGTAAAGGAGAAGAACTTTTCA	To remove RBS sequence from pTn7-M-PEM7-GFP by Gibson Assembly. This work
Tn7-PEM7-R	AACTCCAGTGAAAAGTTCTTCTCCTTTACTCAT ATGTTTTAAGCTTGCATGCCTGCAGGTCG	To remove RBS sequence from pTn7-M-PEM7-GFP by Gibson Assembly. This work
PEM7-F	AATACGACAAGGTGAGGAAC	To amplify and sequence from P_{EM7} promoter. This work
PP5408-F	CGATTCATCAGGTTGGATTCG	To amplify and sequence mini-Tn7 insertions from PP_5408 locus of *P. putida*. This work
Tn7-GlmS	AATCTGGCCAAGTCGGTGAC	To amplify and sequence mini-Tn7 insertions from *glmS* gene of *P. putida* (Lambertsen et al., 2004)
PS2	GCGGCAACCGAGCGTTC	To amplify and sequence from T_0 terminator (Silva-Rocha et al., 2013)
ME-I-Gm-ExtR	GTTCTGGACCAGTTGCGTGAG	To amplify and sequence from mini-Tn7 Gm resistance gene

		(Martinez-Garcia et al., 2014)
RBS-C$_6$	TCTAGAGTCGACCTGCAGGCATGCAAGCTTAGGAGGAAAAACATATGAGTAAAGGAGAAGAACTTTT	Recombineering oligo to insert a consensus 6 nucleotide RBS sequence upstream the *gfp* gene in strains Tn*7*-M-P$_{EM7}$-*gfp*-RBS^{-}. This work
RBS-Deg$_6$	TCTAGAGTCGACCTGCAGGCATGCAAGCTTRRRRRRAAAAACATATGAGTAAAGGAGAAGAACTTTT	Recombineering oligo to insert a degenerated (R=A,G) 6 nucleotide RBS sequence upstream the *gfp* gene in strains Tn*7*-M-P$_{EM7}$-*gfp*-RBS^{-}. This work
RBS-C$_9$	TCTAGAGTCGACCTGCAGGCATGCAAGCTTTAAGGAGGTAAAAACATATGAGTAAAGGAGAAGAACTTTT	Recombineering oligo to insert a consensus 9 nucleotide RBS sequence upstream the *gfp* gene in strains Tn*7*-M-P$_{EM7}$-*gfp*-RBS^{-}. This work
RBS-Deg$_9$	TCTAGAGTCGACCTGCAGGCATGCAAGCTTTARRRRRRTAAAAACATATGAGTAAAGGAGAAGAACTTTT	Recombineering oligo to insert a degenerated (R=A,G) 9 nucleotide RBS sequence upstream the *gfp* gene in strains *Tn7*-M-P$_{EM7}$-*gfp*-RBS^{-}. This work

[a] Asterisks denote phosphorothioate bonds. Single changes introduced by recombineering oligonucleotides SR, NR, RR and PR are highlighted in bold. The three stop codons inserted by oligo CR appear in blue. The sequences encompassing the stretch inserted by the four RBS-X oligos are shown in red color.

SUPPLEMENTARY TABLE S2. Bacterial strains and plasmids used in this work (related to Fig. 2 of main text)

Strain or plasmid	Relevant characteristics [a]	Reference or source
Escherichia coli		
CC118	Cloning host; Δ(*ara-leu*) *araD* Δ*lacX74 galE galK phoA thiE1 rpsE*(Sp^R) *rpoB*(Rif^R) *argE*(Am) *recA1*	(Manoil and Beckwith, 1985)
HB101	Helper strain used for conjugation; F$^-$ λ$^-$ *hsdS20*(rB$^-$ mB$^-$) *recA13 leuB6*(Am) *araC14* Δ(*gpt-proA*)62 *lacY1 galK2*(Oc) *xyl-5 mtl-1 thiE1 rpsL20*(Sm^R) *glnX44* (AS)	(Boyer and Roulland-Dussoix, 1969)
CC118λpir	CC118, λpir lysogen	(Herrero et al., 1990)
Pseudomonas putida		
EM42	KT2440 derivative; Δprophage1 Δprophage4 Δprophage3 Δprophage2 ΔTn7 Δ*endA-1* Δ*endA-2* Δ*hsdRMS* Δflagellum ΔTn*4652*	(Martinez-Garcia et al., 2014)
TA238	EM42 derivative; *rpsL*$^-$(Sm^R) *gyrA*$^-$(Nal^R) *rpoB*$^-$(Rif^R) *pyrF*$^-$(5FOA^R) *catA*-I$^-$	This work
TA245	EM42 derivative with mini-Tn*7*-M-P$_{EM7}$-*gfp*-RBS$^-$ transposon inserted in the *att*Tn*7* site	This work
Plasmids		
pSEVA2314	Inducible expression vector; *oriV*(pBBR1); cargo [P$_L$/cI857]; standard multiple cloning site; Km^R	(Aparicio et al., 2019a)
pSEVA2214-*rec2-mutL*$_{E36K}^{PP}$	pSEVA2214 derivative bearing the *rec2* recombinase and *mutL*$_{E36K}^{PP}$ allele ; *oriV*(RK2); cargo [*c*I857-P$_L$ → *rec2-mutL*$_{E36K}^{PP}$]; Km^R	This work GenBank nº MN688223
pSEVA2314-*rec2-mutL*$_{E36K}^{PP}$	pSEVA2314 derivative bearing the *rec2* recombinase and *mutL*$_{E36K}^{PP}$ allele ; *oriV*(pBBR1); cargo [P$_L$/cI857→ *rec2-mutL*$_{E36K}^{PP}$]; Km^R	This work GenBank nº MN688222

pSEVA2514-*rec2*-*mutL*$_{E36K}^{PP}$	pSEVA2514 derivative bearing the *rec2* recombinase and *mutL*$_{E36K}^{PP}$ allele ; *oriV*(RFS1010); cargo [*c*I857-P_L → *rec2*-*mutL*$_{E36K}^{PP}$]; Km^R	(Aparicio et al., 2019b) GenBank nº MN180222
pSEVA637	*oriV*(pBBR1); cargo [*gfp*]; Gm^R	(Silva-Rocha et al., 2013) (Martinez-Garcia et al., 2015)
pSEVA237R-PEM7	*oriV*(pBBR1); cargo [P_{EM7} → *mCherry*]; Km^R	(Silva-Rocha et al., 2013) (Martinez-Garcia et al., 2015)
pSEVA237-PEM7	*oriV*(pBBR1); cargo [P_{EM7} → *gfp*]; Km^R	This work
pTn7-M	*oriV*(R6K); mini-Tn7 transposon; standard multiple cloning site; Km^R Gm^R	(Zobel et al., 2015)
pTn7-M-PEM7-GFP	pTn7-M derivative with P_{EM7}-*gfp* in the mini-Tn7 transposon; *oriV*(R6K); Km^R Gm^R	This work
pTn7-M-PEM7-GFP-RBS$^-$	pTn7-M-PEM7-GFP derivative lacking the *gfp* RBS; *oriV*(R6K); Km^R Gm^R	This work
pRK600	Helper plasmid used for conjugation; *oriV*(ColE1), RK2 (mob$^+$ tra$^+$); Cm^R	(Kessler et al., 1992)
pTNS2	Helper plasmid for mini-Tn7 transposition; *oriV*(R6K), TnsABC+D specific transposition pathway; Ap^R	(Choi et al., 2005)

[a] Antibiotic markers: Ap, ampicillin; Cm, chloramphenicol; Km, kanamycin; 5FOA, 5-fluoro-orotic acid; Gm, gentamicin; Nal, nalidixic acid; Rif, rifampicin; Sm, streptomycin; Sp, spectinomycin.

SUPPLEMENTARY TABLE S3. Main features of recombineering oligonucleotides used in this study (related to Fig. 2 of main text)

Name	P-thioate bonds	Length	Target gene	Change/mismatch	MMR sensitivity	ΔG (kcal/mol)	Phenotype
SR	Four at 5´-end	94	*rpsL*	A→C/A:G	Low	- 20.79	Sm^R
NR	None	65	*gyrA*	G→A/ G:T C→T/ C:A	High	- 11.84	Nal^R
RR	None	60	*rpoB*	A→T/ A:A	High	- 7.26	Rif^R
PR	None	81	*pyrF*	G→T/ G:A	Low	- 14.03	$5\text{-}FOA^R/Ura^-$
CR	None	89	*catA*-I	Insertion 3 Stops	Low	- 12.84	Catechol accumulation (Brown color)
RBS-C_6	None	67	*gfp* UTR	Insertion 7 nt	Low	- 4.94	Fluorescent
RBS-Deg_6	None	67	*gfp* UTR	Insertion 7 nt (deg.)	Low	Variable	Fluorescent
RBS-C_9	None	70	*gfp* UTR	Insertion 10 nt	Low	- 4.59	Fluorescent
RBS-Deg_9	None	70	*gfp* UTR	Insertion 10 nt (deg.)	Low	Variable	Fluorescent

REFERENCES

Aparicio, T., de Lorenzo, V., and Martinez-Garcia, E. (2019a) Improved thermotolerance of genome-reduced *Pseudomonas putida* EM42 enables effective functioning of the P_L /cI857 System. *Biotechnol J* **14**: e1800483.

Aparicio, T., Jensen, S.I., Nielsen, A.T., de Lorenzo, V., and Martinez-Garcia, E. (2016) The Ssr protein (T1E_1405) from *Pseudomonas putida* DOT-T1E enables oligonucleotide-based recombineering in platform strain *P. putida* EM42. *Biotechnol J* **11**: 1309-1319.

Aparicio, T., Nyerges, A., Nagy, I., Pal, C., Martinez-Garcia, E., and de Lorenzo, V. (2019b) Mismatch repair hierarchy of *Pseudomonas putida* revealed by mutagenic ssDNA recombineering of the *pyrF* gene. *Environ Microbiol* doi: 10.1111/1462-2920.14814.

Boyer, H.W., and Roulland-Dussoix, D. (1969) A complementation analysis of the restriction and modification of DNA in *Escherichia coli. J Mol Biol* **41**: 459-472.

Choi, K.H., Gaynor, J.B., White, K.G., Lopez, C., Bosio, C.M., Karkhoff-Schweizer, R.R., and Schweizer, H.P. (2005) A Tn7-based broad-range bacterial cloning and expression system. *Nat Methods* **2**: 443-448.

Galvao, T.C., and de Lorenzo, V. (2005) Adaptation of the yeast URA3 selection system to Gram-negative bacteria and generation of a Δ*betCDE Pseudomonas putida* strain. *Appl Environ Microbiol* **71**: 883-892.

Herrero, M., de Lorenzo, V., and Timmis, K.N. (1990) Transposon vectors containing non-antibiotic resistance selection markers for cloning and stable chromosomal insertion of foreign genes in gram-negative bacteria. *J Bacteriol* **172**: 6557-6567.

Jimenez, J.I., Perez-Pantoja, D., Chavarria, M., Diaz, E., and de Lorenzo, V. (2014) A second chromosomal copy of the *catA* gene endows *Pseudomonas putida* mt-2 with an enzymatic safety valve for excess of catechol. *Environ Microbiol* **16**: 1767-1778.

Kessler, B., de Lorenzo, V., and Timmis, K.N. (1992) A general system to integrate *lacZ* fusions into the chromosomes of gram-negative eubacteria: regulation of the *Pm* promoter of the TOL plasmid studied with all controlling elements in monocopy. *Mol Gen Genet* **233**: 293-301.

Lambertsen, L., Sternberg, C., and Molin, S. (2004) Mini-Tn7 transposons for site-specific tagging of bacteria with fluorescent proteins. *Environ Microbiol* **6:** 726-32.

Manoil, C., and Beckwith, J. (1985) Tn*phoA*: a transposon probe for protein export signals. *Proc Natl Acad Sci USA* **82**: 8129-8133.

Martinez-Garcia, E., and de Lorenzo, V. (2012) Transposon-based and plasmid-based genetic tools for editing genomes of gram-negative bacteria. *Methods Mol Biol* **813**: 267-283.

Martinez-Garcia, E., Aparicio, T., de Lorenzo, V., and Nikel, P.I. (2014) New transposon tools tailored for metabolic engineering of Gram-negative microbial cell factories. *Front Bioeng Biotechnol* **2**: 46.

Martinez-Garcia, E., Aparicio, T., Goni-Moreno, A., Fraile, S., and de Lorenzo, V. (2015) SEVA 2.0: an update of the Standard European Vector Architecture for de-/re-construction of bacterial functionalities. *Nucleic Acids Res* **43**: D1183-1189.

Ricaurte, D.E., Martinez-Garcia, E., Nyerges, A., Pal, C., de Lorenzo, V., and Aparicio, T. (2018) A standardized workflow for surveying recombinases expands bacterial genome-editing capabilities. *Microb Biotechnol* **11**: 176-188.

Sambrook, J., Fritsch, E.F., and Maniatis, T. (1989) *Molecular cloning: a laboratory manual*. Cold Spring Harbor, NY: Cold Spring Harbor Laboratory Press.

Silva-Rocha, R., Martinez-Garcia, E., Calles, B., Chavarria, M., Arce-Rodriguez, A., de Las Heras, A. et al. (2013) The Standard European Vector Architecture (SEVA): a coherent platform for the analysis and deployment of complex prokaryotic phenotypes. *Nucleic Acids Res* **41**: D666-675.

Zobel, S., Benedetti, I., Eisenbach, L., de Lorenzo, V., Wierckx, N., and Blank, L.M. (2015) Tn7-based device for calibrated heterologous gene expression in *Pseudomonas putida*. *ACS Synth Biol* **4**: 1341-1351.